ZURICH, SWITZERLAND
6 - 10 OCTOBER 2025

EUROPEAN GEOTHERMAL CONGRESS 2025

# Characterizing the subsurface for HT-ATES well design and thermal impact analysis: a case study

Stijn Beernink[1,2], Martin Bloemendal[2,3], Niels Hartog[1,4], Philip J. Vardon[2]

[1] KWR Water Research Institute, Nieuwegein, The Netherlands

[2] Delft University of Technology, Delft, The Netherlands

[3] TNO geological survey, Utrecht, The Netherlands

[4] Utrecht University, Utrecht, The Netherlands

Stijn.beernink@kwrwater.nl

Keywords: HT-ATES, Subsurface characterization, Thermal impact, Recovery efficiency

## ABSTRACT

In this study, well requirements to design the subsurface part of a High Temperature Aquifer Thermal Energy Storage (HT-ATES) are described and assessed for a case-study in Delft (NL). Two recent drillings in Delft are used to design the HT-ATES well. Three main design requirements are identified: flow rate per well, recovery efficiency of the well(s) and the thermal impact to the subsurface. The results of this study show that two layers in Delft between -45 and -184m depth have potential as a storage aquifer for HT-ATES. Because of the higher well flow rate and anticipated smaller thermal impact the deeper storage aquifer is chosen. Based on the flow rate assessment a single doublet should be sufficient to meet the required capacity. Numerical simulations show that the recovery efficiency is 74% after 5 years. The heat losses occur mostly strongly (>50%) towards the top sealing layer, and after five years the thermal energy lost to the shallower layers is greater than the yearly stored thermal energy in the aquifer. The temperature effect, described by monitoring the distance of the +5, +15 and +40 °C temperature increase contours, is two times faster upwards (to shallower layers) compared to deeper layers downwards.

## 1. INTRODUCTION

Large scale seasonal heat storage plays an important role in the energy transition to increase the year round availability of renewable energy (Henry et al., 2020). With High Temperature Aquifer Thermal Energy Storage (HT-ATES), a groundwater well doublet or multiple doublets are used to store large quantities of heat at temperatures relevant for direct heating purposes, e.g. 70 to 100 °C (Bloemendal et al., 2020b). The applicability of HT-ATES is determined by the characteristics of local available aquifers and sealing layers. The design, drilling and materials of the subsurface part of the wells take up a large share of the total capital expenditures of such a system (Zwamborn et al., 2022). To optimize the design and decrease costs, it has to be clear which design requirements should be taken into account and how these properties are determined. In this study, the subsurface hydrogeological properties and layering results of test drillings in Delft, The Netherlands, are used to design a HT-ATES well system. Based on the presented design framework and numerical simulation, generic insights for well design and aquifer characterization for HT-ATES are determined.

## 2. WELL DESIGN REQUIREMENTS AND ASSESSMENT FRAMEWORK

Well design for HT-ATES is aimed to comply with three main characteristics of the HT-ATES system: ensure enough flow rate (loading and unloading capacity) of the system, sufficient heat recovery and prevent excessive thermal impact (Table 1).

### 2.1 Flow rate and capacity

The maximal flow rate ($m^3/h$) of wells is determined by 1. the length of the well screen (m), 2. the designed allowable maximum flow speed on the borehole wall (m/s) and 3. the diameter of the well (m) (Bloemendal et al., 2020a).

1. The length of the well screen depends on the thickness of the available storage aquifer layer(s) and the share of suitable screen sections within each layer (clayey or fine sandy layers are often not used to prevent clogging due to fine particles).

2. A maximal permissible entrance velocity at the borehole wall or well screen is generally used in well design for groundwater wells (Houben, 2015). The purpose of this value is among others to minimize the transport of particles from the gravel pack and aquifer towards the well screen to prevent mechanical clogging (decrease specific flow rate in time) and sand production (could harm the pump and well interior). Although not well substantiated by theoretical or experimental observations, critical entrance velocities of water wells are often linked to the permeability of the porous medium, e.g. according to Huisman (1972):

$$v_c = \frac{\sqrt{K}}{30} \quad [1]$$

Where K is the hydraulic conductivity of the porous medium in m/s and $v_c$ the critical entrance velocity in m/s. In the Netherlands for ATES systems specifically, the NVOE-standard has been used, with success, to calculate safe critical entrance velocities in the past two decades (NVOE, 2006):

$$v_c = 2K$$

3. The potential diameter of the well is in practice determined by the technical possible drilling diameter (e.g. generally 0.3m to 1.5m, depending on drilling method and drilling depth). Larger drilling diameters are preferred as they lead to lower entrance velocity at the borehole wall (Houben, 2015). On the other hand, larger drilling diameters take more time and effort and therefore smaller drilling diameters are preferred to minimize costs. The most suitable drilling diameter is therefore the result of a careful trade-off between all aspects above. The total maximum flow rate q ($m^3$/d) per well is subsequently calculated as the product of the screen length L (m), the well bore diameter D (m) and the permissible speed on the borehole wall $v_c$ (m/d).

$$q_{\max} = L \cdot D \cdot v_c \quad [2]$$

For a specified needed flow rate of the entire HT-ATES system per day ($m^3$/d), the needed amount of wells can be calculated by dividing the needed flow rate by the max flow rate per well.

### 2.2 Heat recovery

The recoverable heat after storage depends, next to operational aspects like total storage volume and cut-off temperature, on the dynamics of the stored heat and related heat losses that occur to the subsurface during storage in the aquifer (Buscheck et al., 1983). Above all, to ensure the stored heat stays close to the well screen during storage, a sealing (low permeable) layer above (and preferably also below) the well screen is needed. When this is the case and no serious effect of ambient groundwater flow is expected, heat losses are mainly due to conduction, dispersion and buoyancy-driven flow depending on the storage conditions and the storage geometry. Conduction occurs due to the temperature difference with he surrounding, mechanical dispersion leads to mixing at the thermal front during injection/extraction due to the heterogeneity of the storage aquifer and buoyancy-driven flow occurs due to the density difference between the stored (light) and ambient (heavy) cold water leading to an upward movement of the stored hot water (Beernink et al., 2024; Bloemendal & Hartog, 2018). In most practical cases heat losses are dominated by conduction or by conduction and buoyancy-driven flow (Beernink et al., 2024). The potential for heat losses due to buoyancy-driven flow in the aquifer is smaller when a (horizontally and vertically) low-permeable aquifer is used. Moreover, these effects are decreased when the ratio of the aquifer thickness to the thermal radius ($L/R_{th}$) is relatively small (<1) , either by using a relatively small well screen length/aquifer thickness or by increasing the total yearly storage volume (Beernink et al., 2024).

The energy recovery is assessed by calculating both the absolute and relative amount of recovered energy. The energy recovered from ($E_{out}$) and stored in ($E_{in}$) the aquifer by the HT-ATES well is determined by:

$$E_{out} = q \cdot (T_{hot,out} - T_{natural}) \cdot C_w \cdot dt$$
$$E_{in} = q \cdot (T_{hot,in} - T_{natural}) \cdot C_w \cdot dt \quad [3]$$

Where q is the flow at a certain time interval dt (e.g. $m^3$/s), $T_{hot}$ the temperature of the hot well, $T_{natural}$ the natural temperature of the aquifer and $C_w$ the volumetric heat capacity of water ($4.18 \times 10^6$ J/$m^3$/K). By dividing the total energy recovered by the energy stored the yearly recovery efficiency of the well ($\eta_{well}$) is calculated:

$$\eta_{well} = \frac{\sum E_{out}}{\sum E_{in}} \quad [4]$$

### 2.3 Thermal impact

Thermal impact from the storage aquifer to the surrounding subsurface is the result of the heat losses that occur from the storage aquifer, which accumulate over the years and distribute outwards (vertically and horizontally) into the subsurface around the well screen due to the same heat transfer processes previously described. The thermal impact to shallower layers is influenced by the thickness of the sealing layer above the well screen and the thermal and hydraulic properties of the sealing layer (Heldt et al., 2024).

Two metrics are used in this study to assess the spatial distribution of heat in time and space. Firstly, the energy per layer is calculated as the energy added to the layer relative to the natural temperature of the subsurface layer:

$$E_{layer} = V_{layer} \cdot \left(\overline{T_{layer}} - T_{natural}\right) \cdot C_{bulk} \quad [5]$$

Where $V_{layer}$ is the volume of the layer, $T_{layer}$ the temperature of the layer, $T_{natural}$ the natural temperature of the layer and $C_{bulk}$ the bulk volumetric heat capacity of the porous medium (average of solid and water phase). Alternatively, the thermal impact is monitored as the temperature increase of the subsurface in time. By doing this, the vertical and spatial distance of a certain temperature increase contour away from the well screen is assessed:

$$\Delta T_{x,z,t} = T_{x,z,t} - T_{natural} \quad [6]$$

In Table 1 an overview of the discussed well design requirements which cover the subsurface parts of the HT-ATES design process is given. The demonstrated steps in this HT-ATES study show a single design iteration regarding the subsurface aspects. The next step, which is not part of this study, is a business case analysis. To come to a satisfactory design, an iterative approach between the well design, performance/ impact analysis and business case analysis is needed in practice.

**Table 1: Well design requirements and assessment parameters**

| | Main well design parameters | Assessed by |
|---|---|---|
| Maximal flow rate per well | Screen length (m), permissible speed on borehole wall (m/s), diameter of well (m) | Maximal flow rate ($m^3$/h) |
| Heat recovery | Aquifer thickness (m), hydrogeological and thermal properties | Total heat recovered (TJ), recovery efficiency (-) |
| Thermal impact | Thickness of sealing layers (m), hydrogeological and thermal properties | Total heat in storage and surrounding layers (TJ), Distance of temperature increase contours in time (m) |

## 3. RESULTS DELFT CASE STUDY

Two drillings were conducted in Delft in 2022, one until 200m depth and the other to 499m depth (Vardon et al., 2022). Of both drillings, cuttings were collected and analyzed, a sweep of logging tools was run and for one borehole also unconsolidated cores were taken and analyzed for hydraulic and thermal properties. A selection of this dataset is used here to describe the shallow subsurface to 300m depth. Between 300m to 499m depth no suitable aquifers were detected. The estimated operational conditions of the Delft HT-ATES system are a total yearly storage volume of 500,000 $m^3$/year at an injection temperature of 80 °C.

### 3.1 Subsurface characterization

3.1.1. Subsurface layering

The Gamma Ray (GR) signal obtained in both wells correlate well, showing clear spikes in GR signal at 40-50m, 75-100 and below 180m depth (Figure 1A). This correlates strongly to observation of clay or very silty fine sand in the cuttings (Figure 1B). These clay layers are also observed as dips in the SPR signal (Figure 1A).

Based on the logging information, cuttings description dataset and descriptions of the sampled cores (core sample depths are shown in Figure 1B), the subsurface until 300m depth is divided into 11 layers consisting of coarse – medium sand, fine sand, very silty fine sand and clay (Figure 1C).

3.1.2. Hydrogeological and thermal properties of layers

From the cores, plugs were taken horizontally (perpendicular to core direction, n=48) and vertically (in alignment with core, n=38). The average thermal conductivity per class decreases with decreasing grain size, going from 2.59 W/mK for medium-coarse sand to 1.77 W/mK for clay (Figure 2). The average thermal conductivity is assigned accordingly to the 4 lithological types in the schematized layering that is used in the simulation model (Figure 1C). Other bulk thermal properties are kept constant and are assumed to be equal for all layers ($c_s$= 700 J/kg, $\theta$=0.3, $\rho_s$=2700 kg/$m^3$).

The hydraulic conductivity of the schematized layers follows the average grain size according to the cuttings description in Figure 1B, supplemented with pumping test data from a nearby well on the 123-184m deep aquifer which resulted in ~ 10m/d $K_h$ (Koulidis et al., in prep.) and available information from the Dutch regional subsurface model (TNO, 2019). The following horizontal hydraulic conductivities are used: 20 m/d for medium-coarse sand, 10 m/d for fine sand, 1 m/d for silty sand and 0.01 for the clay layers. For the potential storage aquifers (coarse-medium sand and fine sand) the horizontal hydraulic conductivity appointed is a conservative estimate to prevent overestimation of well capacity. Oppositely for the aquitards, the appointed hydraulic conductivity for the very silty and clay class are assumed relatively large, so the sealing properties of these layers are not overestimated. For all lithologies, a fixed anisotropy factor ($K_h/K_v$) of 5 is used.

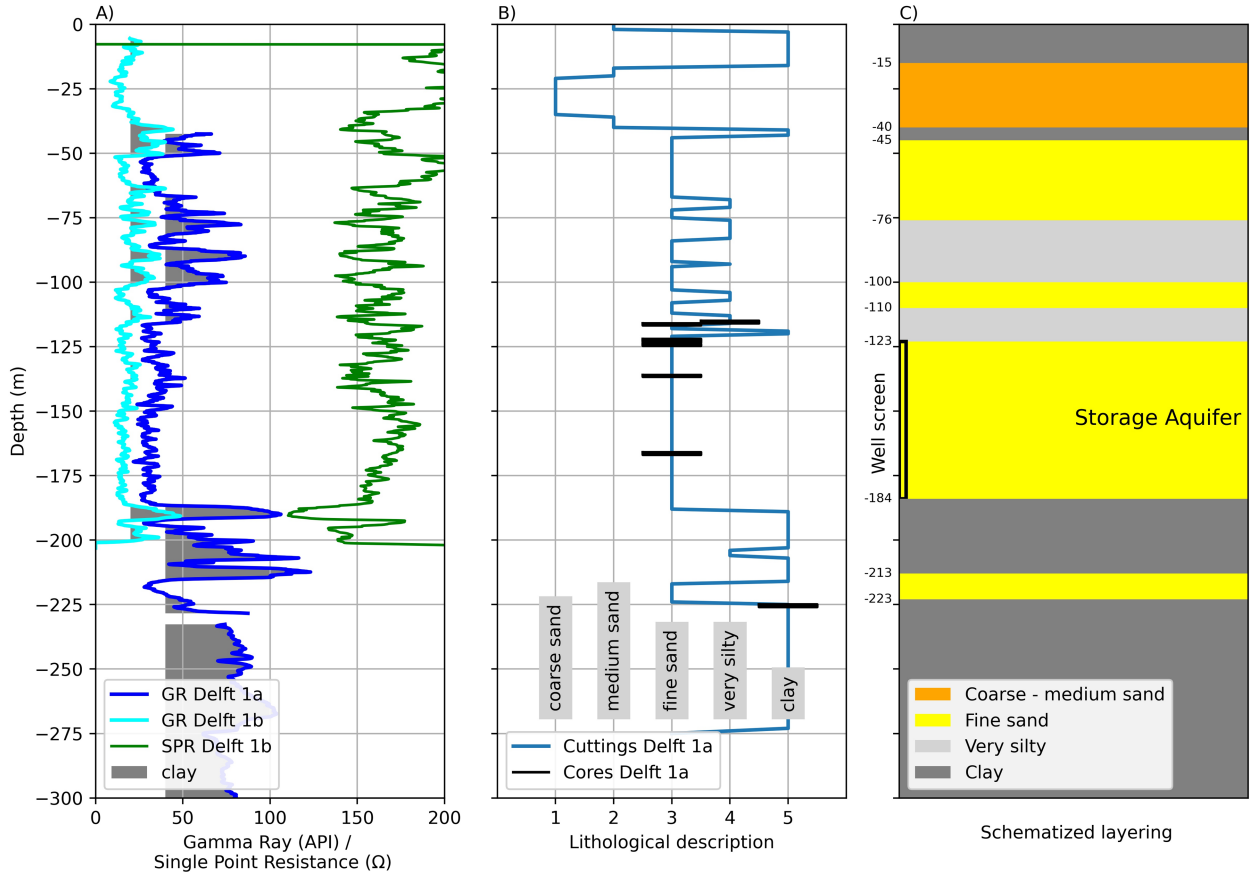


**Figure 1: A) GR and SPR logging data of the two drillings (Delft 1a, Delft 1b). B) Lithological description of the sampled cuttings (each meter) and location of the analysed cores. C) the schematized layering following from the subsurface dataset.**

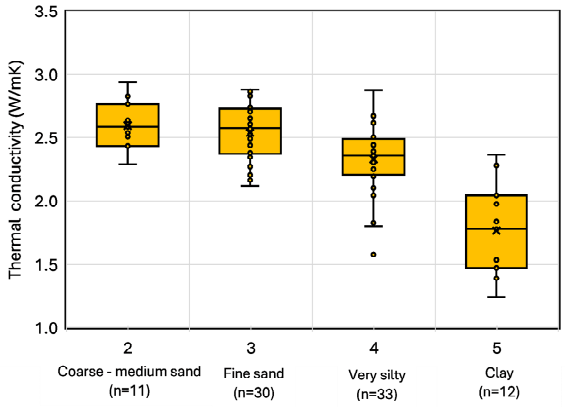


**Figure 2: Measured thermal conductivity (W/mK) of the unconsolidated plug samples from the cores sorted per described lithological class (n=86)**

### 3.2 Well screen placement and designed flow rate

The characterized hydrogeological profile in Delft has two aquifers with a relatively large transmissivity, a shallow aquifer at -45 to -76m (310 $m^2$/d) and a deeper aquifer at -123 to -184m depth (610 $m^2$/d). Advantages of the shallow aquifer are low drilling costs (limited depth) and (expected) suitable aquifer height to minimize heat losses buoyancy-driven, according to the calculated storage geometry (Beernink et al., 2024). Advantages of the deeper aquifer are larger transmissivity (larger well capacity) and the greater depth/thicker sealing layer above which expectedly results in lower potential for unwanted thermal effects to the shallow subsurface. Based on this preliminary assessment, the deeper aquifer is assessed as the aquifer with highest potential for the HT-ATES well screen placement (Figure 1C). Please note that this well design may change again after the assessment of recovery efficiency and thermal impact analysis.

To store the expected yearly storage volume of 500,000 $m^3$ in a half year injection period (150 days) an injection flow rate of 3333 $m^3$/d is needed. This results, based on the Huisman or the NVOE criterium for the measured horizontal hydraulic conductivity of the storage aquifer of ~10 m/d, in a needed well diameter of 0.57 or 0.87m respectively. Hence, based on this criteria, the capacity of a single well using a screen length of 61m should be sufficient to store and extract the needed flow rate of 3333 $m^3$/d.

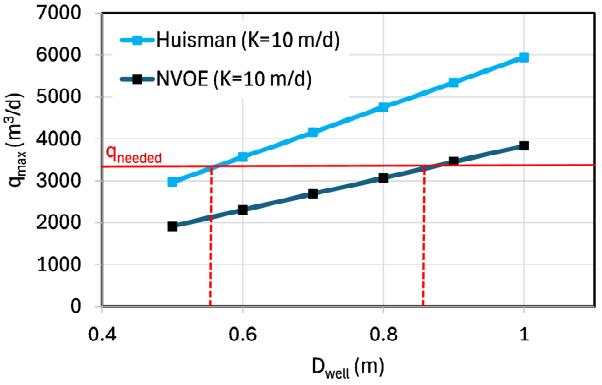


**Figure 3: Calculated maximal flow rate for increasing well diameter ($D_{well}$). To reach the needed flow rate of q=3333 $m^3$/d the well diameter needs to be 0.57m for the Huisman criterium or 0.87m for the NVOE criterium.**

### 3.3 Simulation results

Simulations are done for a single HT-ATES well using an axisymmetric grid setup (meaning that radial symmetry is assumed and hence ambient groundwater flow is neglected), similarly to the approach used in Beernink et al. (2022). The natural temperature of the subsurface is 10 °C for the entire modelling domain. A constant injection flow rate of 3333 $m^3$/d is used for the first 150 days of the year at a constant injection temperature of 80 °C (Figure 4). This is followed by a 30 day storage phase, a 150 day extraction phase (at -3333 $m^3$/d) and a 35 day idle phase at the end of the year. No cut-off temperature is applied during extraction, hence, after a year the net stored volume is zero.

Each year, the temperature drop during extraction decreases as the recovery efficiency increases slightly from 0.736 in the first year to 0.744 in the fifth year. The heat that is stored is situated mostly in the top of the aquifer because of the buoyancy-driven flow due to the density difference between the relatively light hot water and dense cold water (Figure 5). When the aquifer is fully loaded after 150 days of injection the thermal radius at the top of the aquifer (~100m) is about two times the thermal radius of the stored heat at the bottom of the aquifer (~50m).

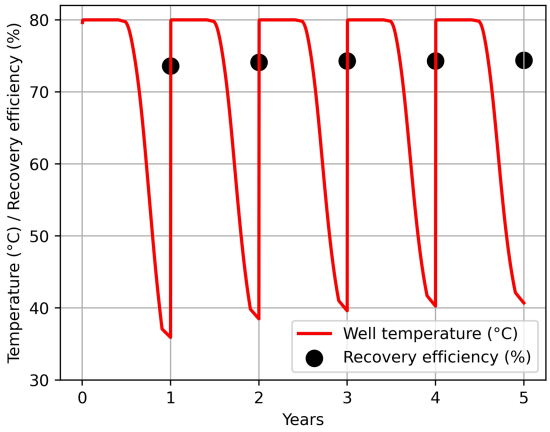


**Figure 4 The simulated well temperature during injection (80 °C) and extraction and the resulting recovery efficiency per year for the simulated 5 year period.**

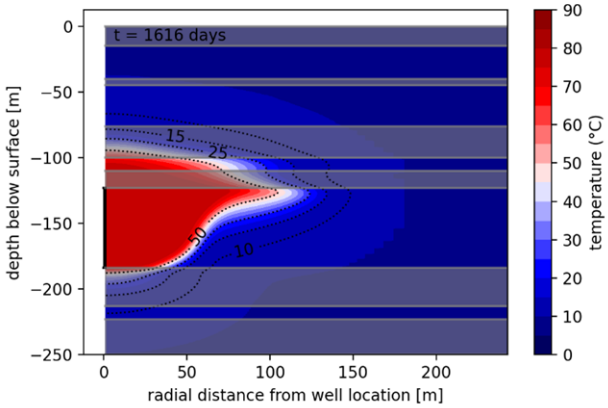


**Figure 5: Cross-section of the temperature in the aquifer and surrounding after full loading (t= 1616 days) in the fifth year.**

As a share of the yearly stored heat is lost to the surroundings, the total amount of energy stored in the subsurface doubles from the first year of HT-ATES operation (~150 TJ) to about 300 TJ in the fifth year of operation (Figure 6). The total energy stored is distributed into the storage aquifer, the layers above the storage aquifer and the layers below the storage aquifer. The energy stored in the layers above the storage aquifer is much higher (100 TJ after five years) than the energy stored in the layers below the storage aquifer (~4 TJ after five years). The extra energy that is left after each subsequent year compared to the previous year is decreasing for the storage aquifer with each year, and is increasing with each year for the layers above. As a result, after the HT-ATES well is fully unloaded at the end of the fifth year, the accumulated energy in the layers above is larger than the energy stored in the aquifer (90 TJ).

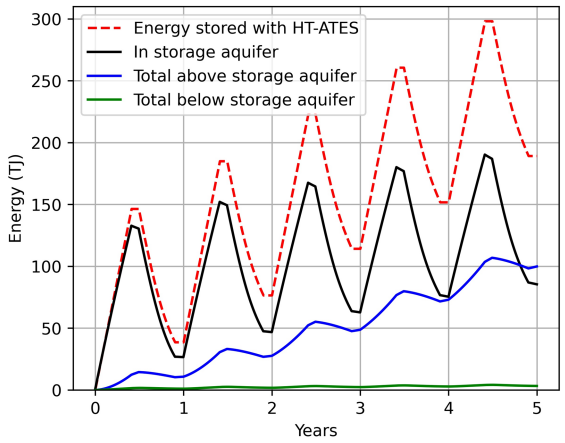


**Figure 6: Energy stored with the HT-ATES and the distribution of the energy in the subsurface layers**

In time, the width of the mixed thermal front and hence the distance between the +40, +15 and +5 °C increases due to mainly conduction (Figure 7). The radial maximal distance of the contours is reached at the top of the aquifer because of the buoyancy-driven flow towards the top of the aquifer (Figure 5). The maximal distance that the contours reach are already much further than the thermal radius that would be expected for a theoretical sharp front without heat transfer:

$$R_{th} = \sqrt{\frac{C_w V_{injected}}{\pi L_{aq} C_{aq}}} \quad [7].$$

Where $C_w$ is the volumetric heat capacity of water, $V_{injected}$ the cumulative sum of the water injected, $L_{aq}$ the aquifer thickness and $C_{aq}$ the bulk volumetric heat capacity of the aquifer.

After 5 years, the maximal distance of the +5 °C contour is already 2 times the $R_{th}$ (140 compared to 65m radial distance from the well screen, Figure 7A). After the first three years the speed of the temperature contour increase seems to decelerate.

Vertically, the temperature increase as a result of the heat losses are both upward and downwards into the sealing layers (Figure 7B). Upward, the temperature contour increase is about two times faster (minimal depth of contour, Figure 7B) compared to the downward speed (maximal depth of contour, Figure 7B). During injection, the thermal radius increases and vertical heat transfer occurs due to conduction both upwards and downwards into the sealing layers. Due to the tilted shape of the stored heat, a much larger surface area of high temperature is situated at the top of the aquifer which results in more and stronger vertical upward conduction. Moreover, next to the larger surface area, also the period that this plume of heat at the top of the aquifer is present is longer (almost entire year) with a radius of minimally 50m (Figure 7A). Oppositely at the bottom of the aquifer, quite soon after the start of extraction no more heat is present at the bottom of the well screen (Figure 7B, +40 °C maximal depth moves upward in the aquifer). Groundwater at a temperature close to the natural groundwater temperature (10 °C) is sucked in again which cools the previously heated bottom clay layer, resulting in decreasing temperature effects downwards.

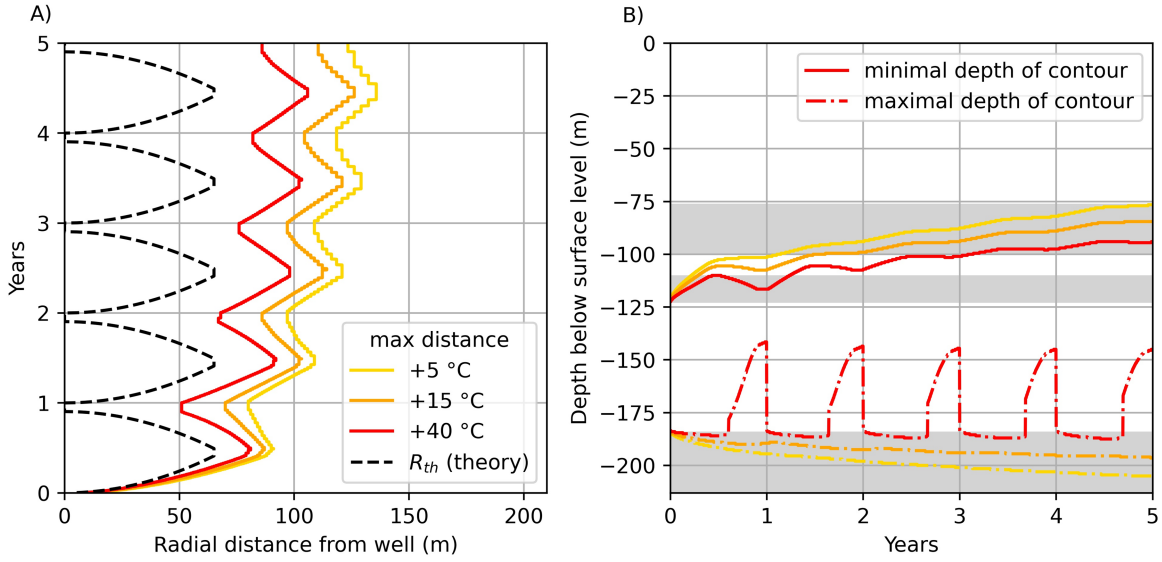


**Figure 7: Distance of the temperature contours of +5, +15 and +40 °C (15, 25, 50 °C) in the subsurface around the well in year 1 to 5 for A) maximal radial distance (at top of storage aquifer) compared to the theoretical thermal radius $R_{th}$ and B) maximal and minimal vertical depth of the contours starting from the well screen top and bottom (123-184m depth).**

## 4. DISCUSSION & CONCLUSIONS

### 4.1 Aquifer characterization and well design

The aquifer with the top at 123m depth was chosen as the storage aquifer in this well design case study. The well capacity of a well in this aquifer is relatively high which limits drilling costs, and also the resistance of the layers above and below is sufficient to hydraulicly seal the aquifer. However, the increase in recovery efficiency of 1 % during the first 5 years is limited (Figure 4), indicating that the performance of the HT-ATES system may stay similar across the lifetime of the HT-ATES. Buoyancy-driven flow seems to be the major reason for the heat losses (Figure 5). To improve the well design, one possibility is to re-assess the hydrogeological characterization, e.g. by gathering more detailed information or re-analysing the existing data. For this case-study, the bulk hydraulic conductivity of the storage aquifer is already quite well known (~10 m/d). However, the (bulk upscaled) anisotropy of the aquifer is estimated a factor 5 and could be much larger if thin, laterally extensive, low permeable layers are included in the analysis, decreasing the effect of buoyancy-driven flow and increasing the thermal recovery efficiency. Alternatively, the suitability of the shallow aquifer at -45 to -76m depth could be investigated. The potential thermal impacts associated with the relatively shallow storage depth are likely to be a challenge.

### 4.2 Thermal impacts

The thermal impacts for the simulated system are almost entirely towards the above sealing layers (Figure 6). While the radial temperature effects seem to stabilize after the first five years (Figure 7A), the upward temperature effects continues steadily (and even seems to increase) during the simulated five year period (Figure 7B). Firstly, an explanation of the relatively strong upward thermal effects might be that the effect is not solely due to heat conduction, but also partly due to advection into the clay layer close to the well screen, because the difference between the hydraulic conductivity of the storage aquifer and the very silty sealing layer (1 versus 10 m/d) is relatively small. However during extraction the opposite happens, the net effect is not well known. Secondly, the strong upward impact is also caused by the buoyancy-driven flow in the aquifer, resulting in the continuous presence of hot water at the top of the aquifer, resulting in strong upward conduction losses. Additionally, as the above sealing layer heats more, buoyancy-driven flow also starts to occur in the highly permeable sandy layer above the storage layer (-100 to -110m depth), which most likely increases the upward heat flux.

### 4.3 Cost-effective method to characterize shallow subsurface combined with geothermal drilling

Aquifer characterization is generally a costly exercise because of high drilling costs and needed efforts. The first stage of a geothermal drilling is often the placement of the conductor and the surface casing, e.g. the first part of the geothermal well that has a relatively large diameter and should function as a steady starting point for the geothermal drilling rig and to acts as a safety barrier between the drilling and the shallow subsurface.

The study of Bloemendal and Beernink (2023) showed that the drilling of the conductor is also easily and cost-effectively used to characterize the shallow subsurface layers in detail (in this case with a water well suction drilling technique). In their study, the drilling of the conductor was made useful for HT-ATES by increasing the drilling depth (extra 130m) inside the conductor with a relatively small drilling depth (300mm). From this deeper drilling inside the conductor detailed cuttings (per m) additional logs and some unconsolidated cores were taken. This method proved to be successful and shows potential for future geothermal – HT-ATES projects.

## 5. CONCLUSIONS

In this study, well design requirements for the subsurface part of a HT-ATES case-study is presented and assessment parameters to check the requirements are described. For the Delft case-study, an assessment of the flow rate, the recovery efficiency and the thermal impact is done, which shows that the subsurface in Delft has potentially suitable aquifers for HT-ATES. Based on the available data, collected with two drillings in Delft in 2022, the subsurface in Delft is characterized and divided into 11 distinctive layers with two layers potentially interesting for HT-ATES. The deepest aquifer, between 123m and 184m depth is chosen as the most suitable aquifer because of the relatively large capacity per well (only one hot well needed of ~ 0.5 – 0.8m diameter to accommodate the total needed flow rate of 500,000 $m^3$ per year).

The simulated recovery efficiency of the well in the fifth year is reasonable at 74% but does not show much improvement over the years. The thermal impact that is simulated is analysed in this study by monitoring the energy distribution in time and the radial/vertical distance of the +5 °C, +15 °C and +40 °C temperature contours relative to the well screen in time. Most thermal impact occurred towards the above layers above the storage aquifer an after the five year simulated period more heat was lost to the shallower layers than stored yearly in the aquifer. Well design could be improved by re-assessing the hydrogeological properties of the chosen aquifer and the sealing layers (e.g. anisotropy ratio). Alternatively, the suitability of the shallow aquifer at -45 to -76m depth could be investigated. The potential thermal impacts associated with the relatively shallow storage depth are likely to be a challenge. In practice, HT-ATES design is an iterative process involving well design, analysis of subsurface performance and business-case analysis.

## REFERENCES

Beernink, S., Barnhoorn, A., Vardon, P. J., Bloemendal, M., & Hartog, N. (2022). *Impact of vertical layering and the uncertainty and anisotropy of hydraulic conductivity on HT-ATES performance*. Paper presented at the European Geothermal Congress 2022, Berlin.

Beernink, S., Hartog, N., Vardon, P. J., & Bloemendal, M. (2024). Heat losses in ATES systems: The impact of processes, storage geometry and temperature. *Geothermics, 117*, 102889. doi:https://doi.org/10.1016/j.geothermics.2023.102889

Bloemendal, M., & Beernink, S. (2023). *HT-ATES feasibility for TRIAS Westland: case study* (KWR.2022.125). Retrieved from Nieuwegein: https://mp.watereurope.eu/media/publications/KWR2022.125_HT-ATES_triasWestland_feasibility.pdf

Bloemendal, M., & Hartog, N. (2018). Analysis of the impact of storage conditions on the thermal recovery efficiency of low-temperature ATES systems. *Geothermics, 17*, 306-319. doi:10.1016/j.geothermics.2017.10.009

Bloemendal, M., Lopik, v. J., Jansen, J. H. F., Drijver, B., Bergen, v. F., Koenen, M., . . . Khoshnevis, N.

(2020a). *Literatuurstudie Brontechniek | WINDOW werkpakket C1*. Retrieved from Nieuwegein:

Bloemendal, M., Vardon, P. J., Medema, A., Snelleman, S., Marif, K., Beernink, S., . . . Van Oort, T. (2020b). *Feasibility study HT-ATES at the TU Delft campus*. Retrieved from https://www.warmingup.info/documenten/window-fase-1---a1---verkenning-hto-tud---feasibilityht_ates_tudelft.pdf

Buscheck, T. A., Doughty, C., & Tsang, C. F. (1983). Prediction and analysis of a field experiment on a multilayered aquifer thermal energy storage system with strong buoyancy flow. *Water Resources Research*, *19*(5), 1307-1315. doi:10.1029/WR019i005p01307

Heldt, S., Beyer, C., & Bauer, S. (2024). Uncertainty assessment of thermal recovery and subsurface temperature changes induced by high-temperature aquifer thermal energy storage (HT-ATES): A case study. *Geothermics*, *122*, 103086. doi:https://doi.org/10.1016/j.geothermics.2024.103086

Henry, A., Prasher, R., & Majumdar, A. (2020). Five thermal energy grand challenges for decarbonization. *Nature Energy*, *5*(9), 635-637. doi:10.1038/s41560-020-0675-9

Houben, G. (2015). Review: Hydraulics of water wells—flow laws and influence of geometry. *Hydrogeology Journal*, 1-25. doi:10.1007/s10040-015-1312-8

Huisman, L. (1972). *Groundwater Recovery and Recharge*: Macmillan.

Koulidis, A., van der schans, M., Vardon, P. J., & Bloemendal, M. (in prep.). *Drilling Report HTO-01 Monitoring Borehole*. Retrieved from Delft:

NVOE. (2006). *NVOE-richtlijnen Ondergrondse Energieopslag*. Retrieved from Woerden: https://branchevereniging.bodemenergie.nl/wp-content/uploads/sites/3/2021/05/NVOE-Werkwijzen-en-richtlijnen-ondergrondse-energieopslag.pdf

TNO. (2019). *Totstandkomingsrapport Hydrogeologisch Model (REGIS II)*. Retrieved from Utrecht:

Vardon, P. J., Laumann, S., Schmiedel, T., Vargas Meleza, L., Barnhoorn, A., Abels, H., . . . van den Berg, J. (2022). *Drilling report: Delftse Hout multipurpose research borehole. DAPGEO-02*. Retrieved from Delft:

Zwamborn, M., Beernink, S., Kleinlugtenbeld, R., Oerlemans, P., Pothof, I., Star, K., . . . Bloemendal, M. (2022). *HT-ATES systems in district heating networks, a Dutch benchmark study*. Paper presented at the European Geothermal Congres, 2022, Berlin.